Radiation Environment Measurements from CREAM and CREDO During the Approach to Solar Maximum

Clive S. Dyer, P. R. Truscott, C. Sanderson, C. Watson, C. L. Peerless, P. Knight, R. Mugford, T. Cousins, and R. Noulty

***Abstract*—Results from the Cosmic Radiation Environment Monitors (CREAM and CREDO) have been reported from a range of platforms during the declining phase of solar cycle 22 and a number of implications drawn for radiation environment and shielding models. Since these reports, the CREAM monitor has flown on a number of Shuttle visits to MIR during 1997–1998 with an extended deployment on MIR during January to May 1998. In all cases an active monitor measured charge-deposition spectra at various locations, while passive packages comprising neutron activation foils, neutron bubble detectors and thermoluminescent dosimeters obtained integrated data at these and other sites. Movement of the South Atlantic Anomaly is observed and cannot be fitted by simply updating the geomagnetic field model. The data from MIR are compared with those from previous Shuttle missions and show comparable secondary neutron fluencies and dose rates. Meanwhile a CREDO-3 particle telescope has been included in the Microelectronics and Photonics Test Bed in highly eccentric, high inclination orbit and has been returning data since November 1997. This experiment measures proton fluxes greater than 38 MeV and linear energy transfer spectra of cosmic rays and solar particle events in the range 100–20 000 MeV/(g cm-2). The data have been extended to July 2000 and are used both to correlate with device behavior and to compare with models of trapped radiation, cosmic rays and solar particles. A number of solar particle events have been observed as cycle 23 builds up. Following a relatively quiet year in 1999, the recent event of July 14, 2000 is observed to compete with the October 1989 events in terms of proton fluency but has a somewhat lower heavy ion fraction.**

I. Introduction

THE CONSTRUCTION of accurate space radiation environment models requires measurements over a range of solar cycle conditions and orbital situations spanning the entire magnetosphere. In addition, the complexities of spacecraft shielding effects require the application of radiation transport codes and the measurement of secondary radiation such as neutrons. In previous papers, results have been presented from the Cosmic Radiation Environment and Activation Monitor (CREAM) and Cosmic Radiation Environment Dosimetry Experiment (CREDO) carried on platforms ranging from aircraft to geostationary orbit during the descending phase of solar cycle 22 between 1990 and early 1997 [1]–[3]. These measurements cover total dose, charge-deposition spectra, linear energy transfer spectra and secondary neutron fluencies.

Manuscript received July 25, 2000.

C. S. Dyer, P. R. Truscott, C. Sanderson, C. Watson, C. L. Peerless, P. Knight, and R. Mugford are with the Space Department, DERA Farnborough, GU14 0LX, England (e-mail: csdyer@scs.dera.gov.uk).

T. Cousins is with Defence Research Establishment, Ottawa, Canada.

R. Noulty is with Bubble Technology Industries, Chalk River, Canada.

Publisher Item Identifier S 0018-9499(00)11248-1.

During the rising phase of solar cycle 23 there have been a number of Shuttle flights of CREAM including an extended duration deployment on the Russian MIR space station. In addition, a new version of CREDO has been deployed as part of the Microelectronics and Photonics Test Bed which has been operating in highly eccentric orbit since November 1997. Results up to July 2000 are presented here.

II. Instruments and Missions

A. CREAM

The CREAM monitor, which comprises both active and passive detectors, has flown on a number of Shuttle missions at a variety of inclinations and altitudes, commencing with STS-48 in September 1991. The active detector employs a planar array of pin diodes combined with pulse-height analysis to measure charge-deposition spectra. The passive detectors include activation foils to measure neutrons and thermoluminescent dosimeters to measure dose. On recent missions these have been complemented by neutron bubble detectors. The most recent paper [4] included data up to the STS-81 mission, which docked with MIR in January 1997. Since then CREAM has flown on four further missions to MIR, namely STS-84 in May 1997, STS-86 in September 1997, STS-89 in January 1998 and STS-91 in June 1998. During the STS-86 mission both active and passive detectors were deployed on MIR for a short duration, while the detectors were operated on MIR for an extended period between delivery by STS-89 and retrieval by STS-91. The active detector was deployed sequentially at two locations. These were chosen with the intention of providing minimum and maximum shielding and are respectively:

i) Base block, floor of Commander's sleep station;
ii) Base block panel 410.

The passive packages were placed at these two locations and at a further three as follows:

iii) Kvant-II close to emergency water tanks;
iv) Kvant-II close to external Particle Interaction Experiment location used between April 1996 and May 1997. [4];
v) Base block panel 323.

B. CREDO-3

CREDO-3 is a miniaturized version of the CREDO series of experiments which have flown on UoSAT's (University of Surrey Satellites), APEX (Advanced Photovoltaics and Electronics Experiment) and STRV (Space Technology Research Vehicle) spacecraft. The main aim is to measure particle fluxes,

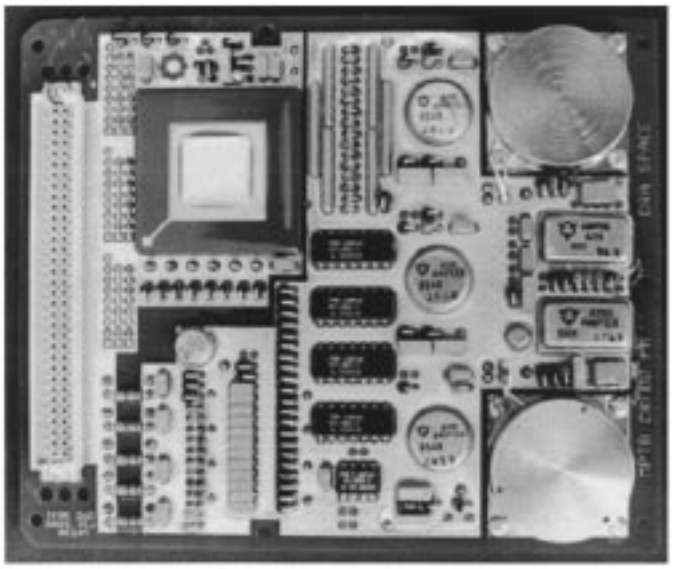

Fig. 1. The CREDO-3 experiment board on MPTB. The proton and ion telescopes are on the right.

charge-deposition spectra and linear-energy-transfer spectra required for the prediction of single event effects and background noise in sensors. Recent results from previous versions have shown important results for environment models [3], [4] as well as correlation with single event upsets and burn-outs [5]. This version has been designed to provide the environment dosimetry for the Microelectronics and Photonics Test Bed [6], which is aimed at space testing a number of advanced technologies in a radiation-stressing, Molniya orbit, which is highly inclined (63°) and elliptic ($39\,200 \times 1200$ km). A description of the instrument and early results has been given in [7].

CREDO-3 is designed to fit onto a single MPTB test board (127×152 mm) and comprises two particle telescopes with pulse-height analysis and a Field Programmable Gate Array (FPGA) interface to the MPTB computer. The FPGA can be seen covered with additional tantalum shielding to give adequate lifetime in the high dose environment. Each telescope comprises two pin diodes each of 3 cm^2 area and separated by 2 cm. A picture of the CREDO-3 board is given in Fig. 1. The depletion depth of the diodes is 380 μm. Both noncoincident (singles) and coincident events are recorded and the latter imply an acceptance cone of half-angle 26.6° and a geometric factor of 1.56 cm^2sr. The latter has been calculated using both analytical and numerical integration methods. Electron events are minimized by a 1.5 mm brass shield, which, in combination with the MPTB box skin, affords a shielding of 1.6 g cm^{-2} in the space direction. The reverse cone is afforded in excess of 30 g cm^{-2} by the spacecraft structure. Hence electrons of energy less than about 2.6 MeV do not penetrate and further elimination is provided by charge-deposition thresholds of 0.4 MeV for the proton monitor and 9 MeV for the ion monitor. Therefore electrons can be detected only by pulse pile-up in very intense flux regimes. This occurs for proton singles in the heart of the outer belt but the ion channels are immune to this contamination. The proton telescope measures fluxes of protons of energy greater than 38 MeV, while the ion monitor measures linear energy transfer (LET) spectra in 16 channels which cover the range from 100 to 20 000 MeV/(g cm^{-2}), with an upper channel providing an integral measurement above the higher level. Data are accumulated into re-programmable time bins with one-minute time resolution used for the data since January 30, 1998 and six-minute resolution for the earlier data obtained following switch-on November 25, 1997. Essentially continuous data coverage has been obtained from switch-on until the present (July 2000) with the exception of a few periods of eclipses at around perigee and other minor data outages.

III. Results

A. CREAM on MIR

1) Active Monitor: In Fig. 2(a), count rates from CREAM channel 1 are shown for the 7th day of CREAM deployment on MIR in January 1998. This channel measures particles with LET > 6.8 MeV/(g cm^{-2}) and its threshold for proton detection is set by the amount of shielding. For the locations in MIR this is in the range 50 to 100 MeV. The upper panel is the total count rate comprising contributions from both cosmic rays and trapped protons. The cosmic-ray contribution varies in anti-correlation with the geomagnetic cut-off rigidity, which is calculated using the update IGRF95 field model and shown in the bottom panel. A fit to the cosmic-ray variation is subtracted from the counts to give the contribution from protons in the South Atlantic Anomaly (SAA) and this is shown in the second panel. Comparison is made with predictions using AP8 in conjunction with the updated field model. The predicted flux of protons of energy greater than 100 MeV is shown in the third panel. It is known that this prediction technique gives erroneous fluencies [8] but in this case the prediction also completely misses a South Atlantic Anomaly pass (the last one in the day). This is further illustrated by the ground track and proton flux contours shown in Fig. 3 where it can be seen that this pass lies to the northwest of the SAA as predicted by simply updating the field. In addition, a pass is predicted but not seen and this lies to the southeast. The SPENVIS code system [9] employs the magnetic field corresponding to the time during which AP8 data were taken and then simply rotates the anomaly westwards by 0.3° per year to allow for field evolution. This technique is found to give improved prediction of belt passes as shown in Fig. 2(b). In order to obtain this result, it was necessary to run SPENVIS with time resolution finer than the default (i.e., 1 minute cf 2 minute). Here the observed rates are converted into an approximate flux by dividing by the omnidirectional geometric factor (2.5 cm^2) and accumulation time (300 seconds). The absolute comparison is only approximate as there is not a clear cut proton energy threshold in the complex shielding situation within MIR. However the predicted fluxes at greater than 100 MeV are within about a factor of two. More importantly all passes are predicted and no spurious passes are predicted. This fix-up to AP8 is not fully satisfactory and will have limited ability to be extrapolated into the future. In addition, the shape of the SAA is changing and cannot simply be treated as a westwards rotation.

There are two modeling efforts in progress to create low altitude proton models. These are based on more recent data from SAMPEX/PET for the solar minimum of 1994–1995 [10] and

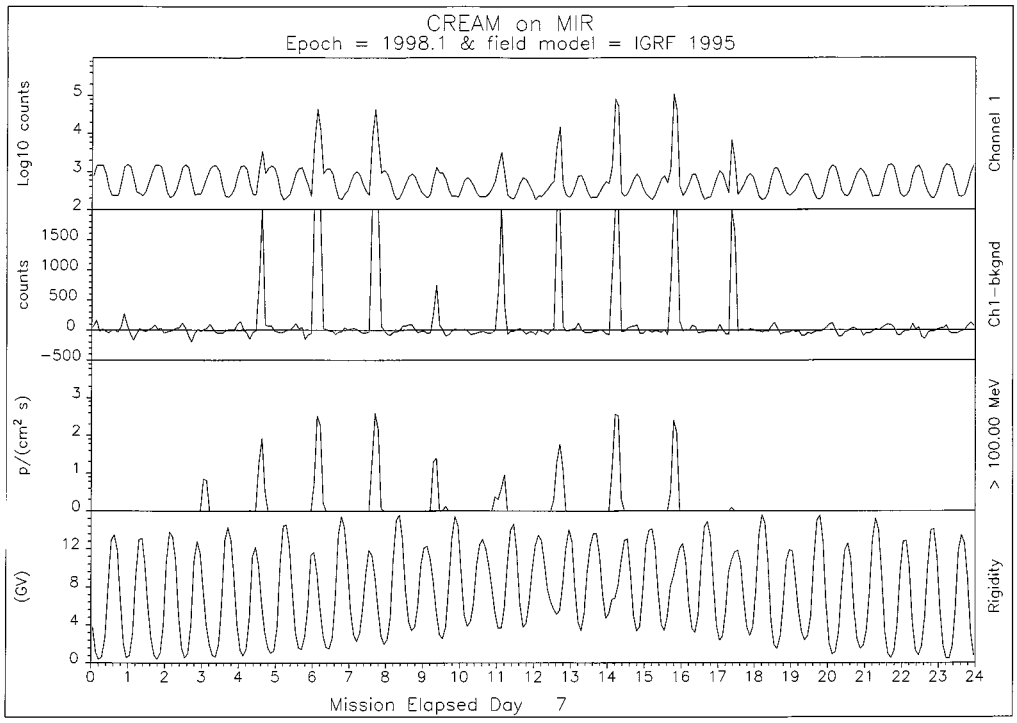

(a)

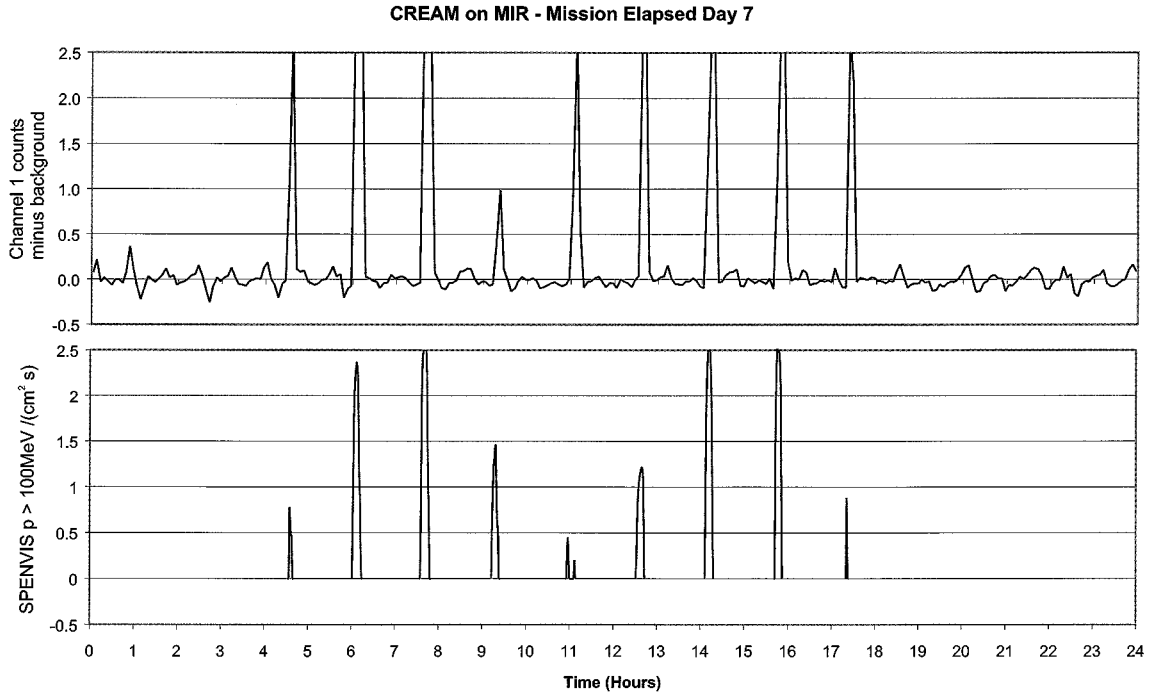

(b)

Fig. 2. (a) Count-rate variations from CREAM on MIR for the 7th day of the mission. The upper panel includes cosmic rays which anti-correlate with the cut-off rigidity shown in the bottom panel. These are subtracted to give the SAA proton contribution shown in the second panel and the result is compared with AP8 predictions in conjunction with the IGRF 1995 field model updated to 1998, as shown in the third panel. This procedure misses an important SAA pass and predicts a pass that is not observed. (b) The SAA count rates from Fig. 2(a) are converted into fluxes and compared with predictions using AP8 in SPENVIS which allows for movement of the SAA. All passes are now predicted and the absolute agreement is reasonable given the uncertainties in shielding and proton threshold.

a twenty year data set obtained from TIROS/NOAA spacecraft since 1978 [11]. It would be valuable to make comparisons with these models but they are not yet generally available. It is notable that data on high energy protons (>100 MeV) are limited while these energies are extremely important for effects within Shuttle and Space Station.

The same CREAM active unit was deployed at two locations on MIR during January–May 1998 as was deployed in SpaceHab on STS-63 during February 1995. In Fig. 4 the charge-deposition spectra obtained in the two MIR locations are compared with those obtained in two SpaceHab locations. These measurement periods were obtained on either side of

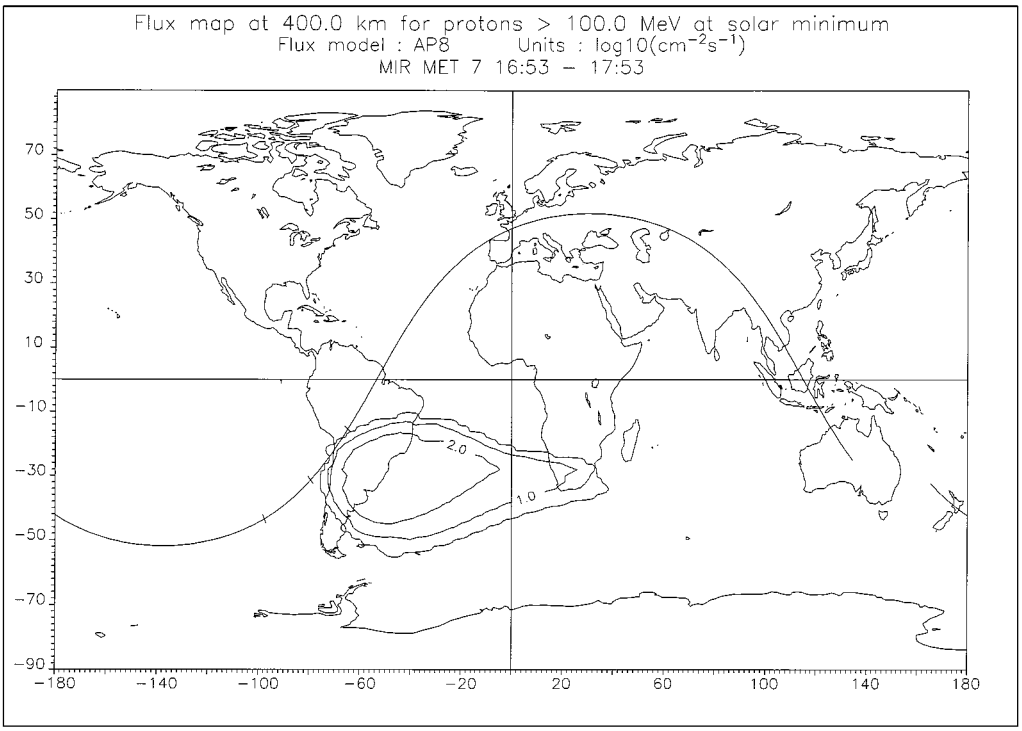

Fig. 3. Ground track for the SAA pass that was not predicted by simply updating the field model (i.e., 1653 to 1753 mission elapsed time on day 7). The flux map is for protons of energy $>$100 MeV at 400 km altitude as calculated using AP8MIN and the updated field. Units are $\log_{10}$ of the flux in cm^{-2} s^{-1}.

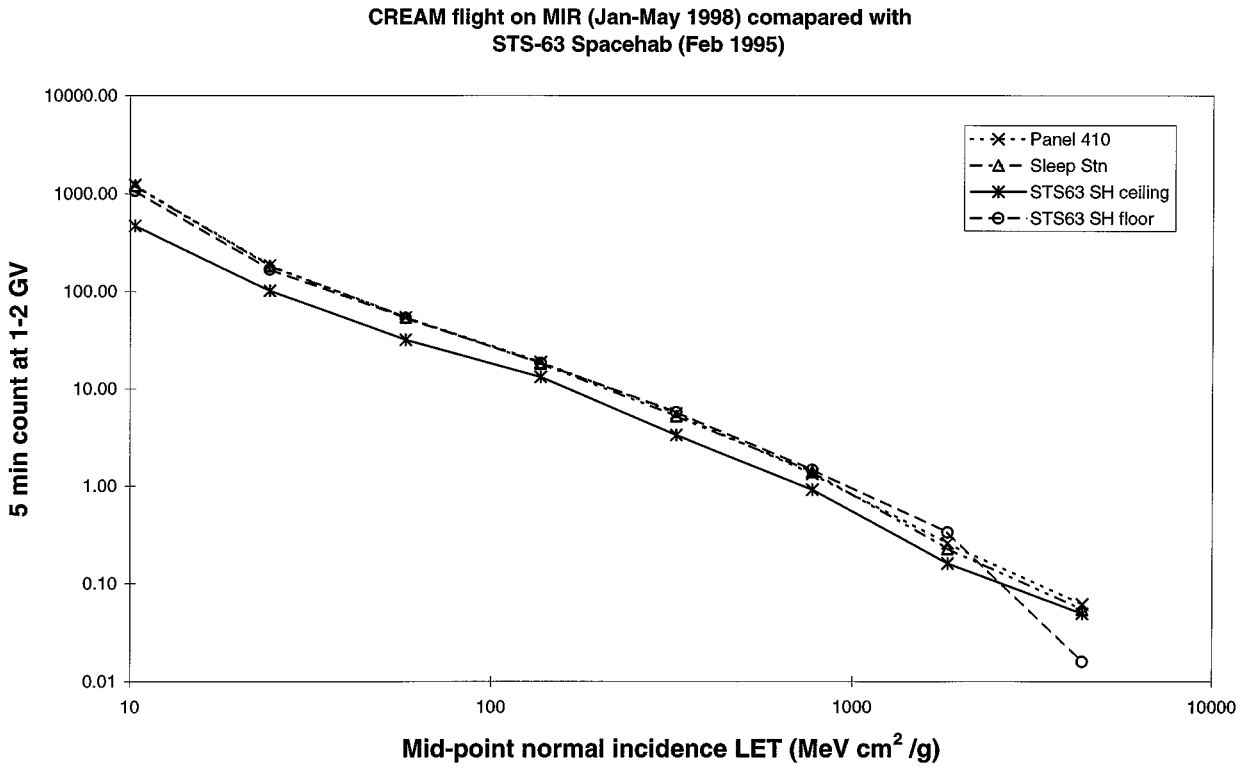

Fig. 4. Charge-deposition spectra at 2 MIR locations (panel 410 and sleep station) in January to May 1998 compared with those obtained in SpaceHab (ceiling and floor) during February 1995. These are periods of similar overall cosmic-ray flux. The lowest intensity is in the minimum shielding location on the SpaceHab ceiling.

solar minimum and cosmic-ray fluxes were very similar (to within 0.6% based on the neutron monitor data from Climax, CO). Although the two MIR locations were chosen to represent shielding extreme there is no discernible difference between them. They also closely match the more highly shielded SpaceHab location (floor). It should be noted that the highest channel has poor statistics, with only one count accumulated for the SpaceHab floor location. For channels below this the

TABLE I
CREAM PASSIVE DETECTOR RESULTS FROM ON BOARD MIR

	STS-89 Long Jan - Jun 98 51.6° 380km			STS-89 Short Jan-98 51.6° 380km
Location	Average dose rate from DERA TLD's [mrad(Si)/day]	Thermal neutron neutron flux from gold foil [$cm^{-2}s^{-1}$]	Fast neutron flux from nickel foil [$cm^{-2}s^{-1}$]	Mean neutron dose from bubble detectors [mrem/day]
Locn#1 (Sleep Station Core Module)	21.8 ± 1.0	0.148 ± 0.056	1.138 ± 0.061	10.5 ± 2.8
Locn#2 (Panel 410)	18.0 ± 2.8	0.176 ± 0.049	1.363 ± 0.074	10.8 ± 3.3
Locn#3 (KVANT-II Water Tanks)	21.2 ± 0.4	0.163 ± 0.055	1.152 ± 0.075	10.5 ± 3.2
Locn#4 (KVANT-II)	26.4 ± 1.2	0.274 ± 0.053	1.151 ± 0.073	9.8 ± 2.2
Locn#5 (Panel 323)	16.6 ± 0.4	0.203 ± 0.049	1.295 ± 0.074	10.5 ± 2.5

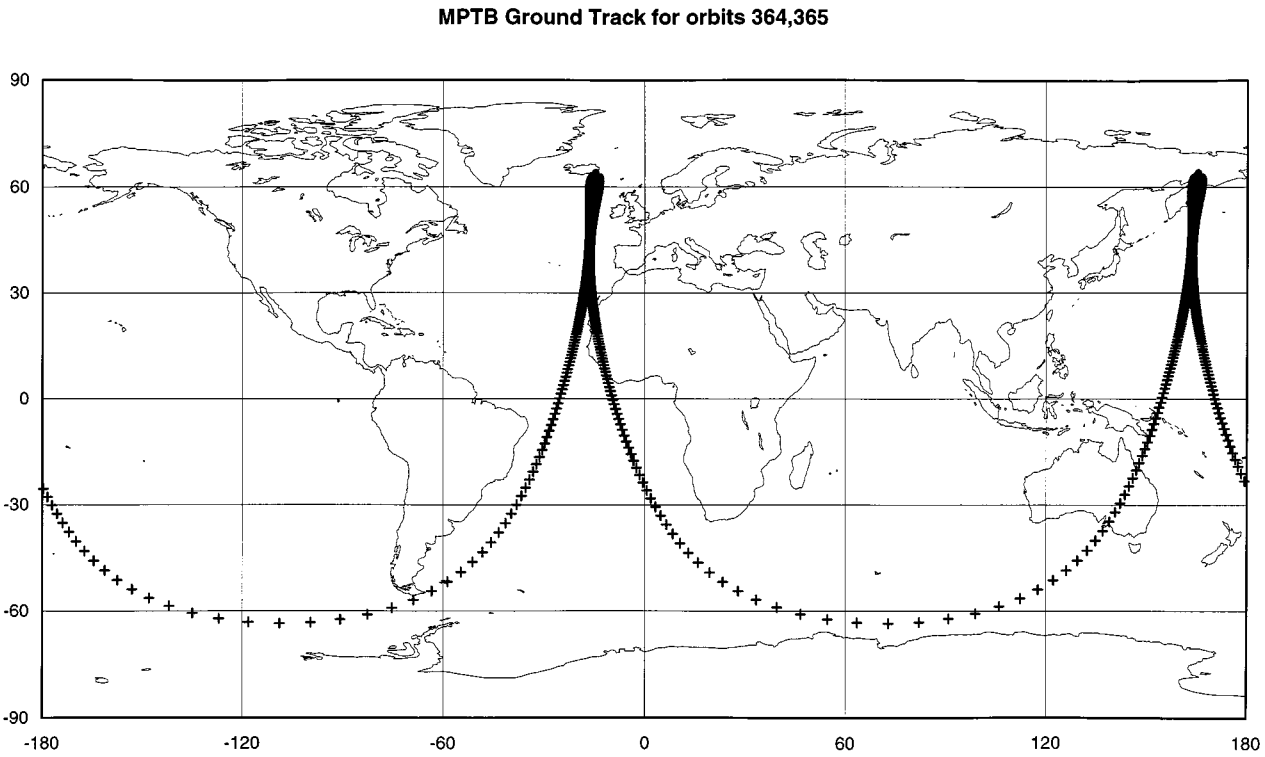

Fig. 5. MPTB ground tracks for orbits 364 and 365. Note that orbit 364 starts at the southwards equator crossing at the right hand end of the figure and then continues to the left showing a perigee in the Southern Pacific. Orbit 365 then commences with the southward equator crossing at around $-10°$ longitude.

statistical errors vary from 20% to 0.5%. Significantly lower measurements were obtained at the lightly shielded SpaceHab ceiling location. This is consistent with the build-up with shielding noted from different Shuttle locations [3].

2) Passive Detectors: Results from various CREAM passive detectors deployed on MIR are presented in Table I. The thermoluminescent dosimeter (TLD) and activation foil data are from the long duration deployment on MIR while the bubble detector data are from a short duration exposure in January 1998. Data from TLD's and activation foils have been presented previously for a wide range of Shuttle missions [3]. The most comparable mission for cosmic-ray intensity and altitude was STS-63 for which very comparable TLD dose rates were obtained in the airlock and wall locations (17.7 and 20.6 mrads per day respectively). The SpaceHab floor measurement on STS-63 was 22.5 while the least shielded SpaceHab ceiling gave the much higher rate of 44.1. Fast neutron fluxes varied between 0.8 and 1.2, while thermal neutron fluxes ranged from 0.08 to 0.15. The previous neutron bubble detector data on neutron dose rates were obtained on STS-81 in January 1997 when dose-rates of 7.4 to 8.0 mrem per day were obtained. In general all rates are very similar between Shuttle and MIR with the exception of higher directly ionizing dose rates at very thin shielding where electrons dominate.

B. CREDO-3 on MPTB

1) Spatial Variations: Data have been plotted on an orbit basis, each being conveniently of 12 hours duration. Differences

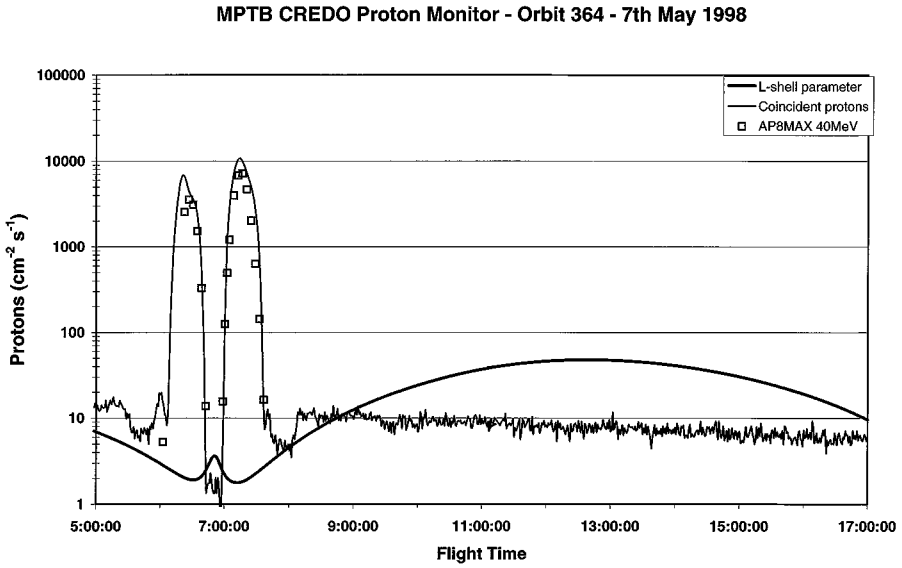

Fig. 6. Time variations of MPTB CREDO proton channel rates around an even orbit (number 364 on May 7, 1998) are compared with geomagnetic L-shell parameter. The two peaks are inner-belt particles while beyond $L = 10$ there is full exposure to cosmic rays. The predicted inner-belt fluxes from AP8MAX in SPENVIS are shown as squares.

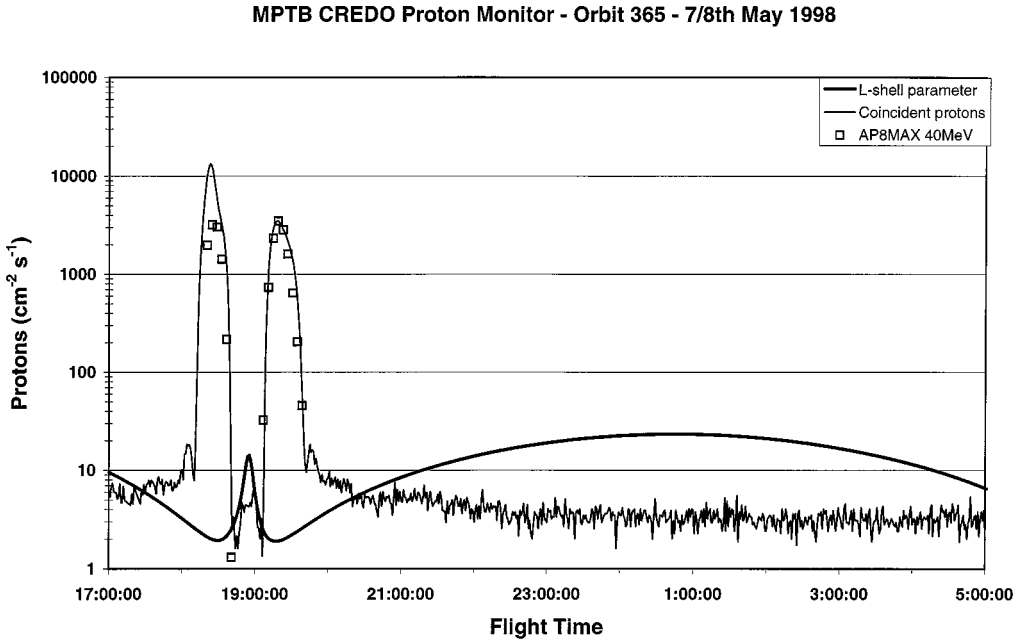

Fig. 7. Time variations for the ensuing odd orbit, number 365 on 7/8 May 1998.

between odd and even numbered orbits occur because of the tilt and displacement of the earth's magnetic field. The ground track of the orbit is given in Fig. 5 for orbits 364 and 365 on May 7 and 8,1998. The measured proton fluxes, together with the geomagnetic L-shell parameter, are presented in Figs. 6 and 7. The L-shell [12] is a measure of the geomagnetic field line on which the spacecraft is situated and may be thought of as the geocentric distance (in earth radii) of the field line in the magnetic equatorial plane. It is employed to order radiation belt data in the various models and it is also related to the rigidity (momentum-to-charge ratio) required by an external cosmic ray in order to be able to penetrate the geomagnetic shielding (to a reasonable approximation, cut-off rigidity for vertical arrival in GV is given by $16/L^2$).

The two peaks are due to passages through the heart of the inner radiation belt on either side of perigee, while for most of the orbit outside of the belts the counts are from cosmic rays and are flat with time as the orbit is fully exposed ($L > 10$; cut-off rigidity <0.16 GV). A slight downward trend is due to the decay of some remaining protons from a solar particle event on May 6th. For the even-numbered orbit, perigee occurs in the South Pacific near South America and although the L-value shows an increase at perigee due to the high latitude, it does not exceed 3. From this perigee position the orbit ascends through the South

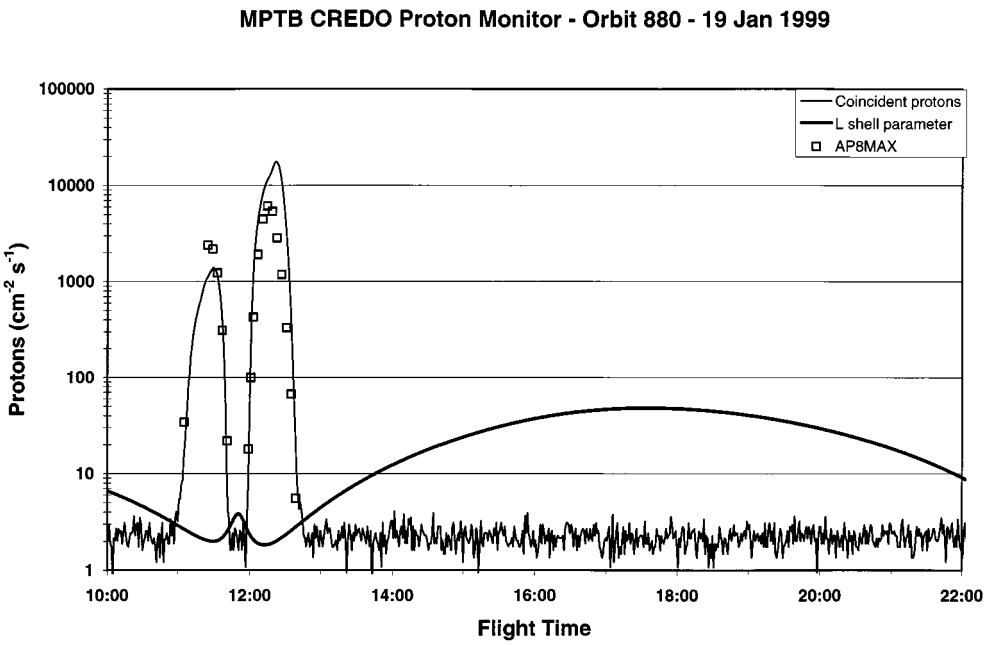

Fig. 8. Later even orbit, number 880 on January 19, 1999.

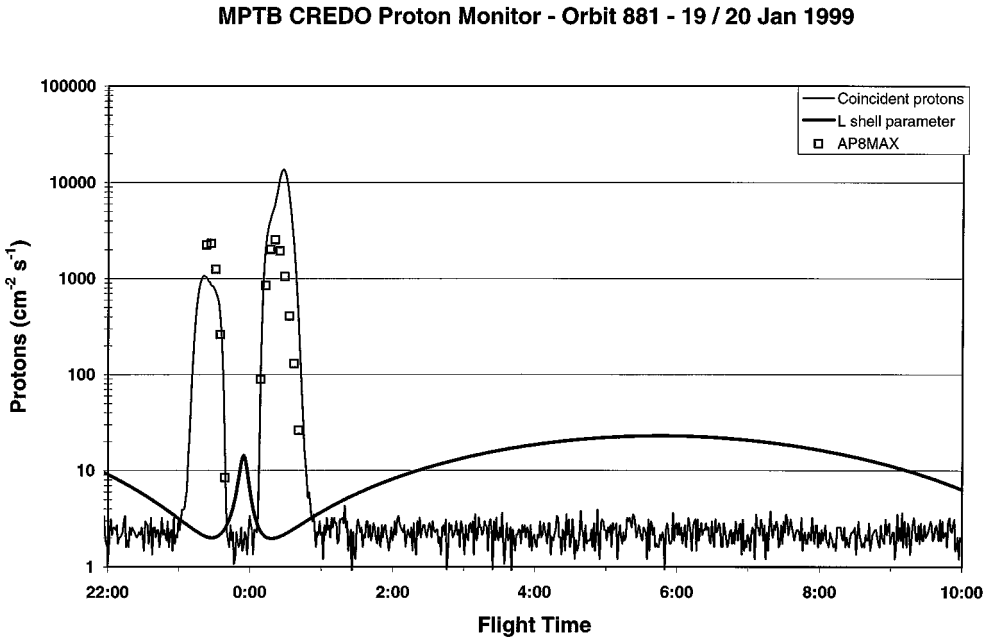

Fig. 9. Later odd orbit, number 881 on January 19 and 20, 1999.

Atlantic region where L-values are low and the trapped protons come lower in altitude. Hence this pass experiences the maximum number of protons.

This is in contrast with the ensuing odd-numbered orbit shown in Fig. 7. Here perigee occurs in the Southern Ocean near to the south magnetic pole and so higher L-shells are reached ($L > 10$). This difference means that even-numbered orbits experience more inner-belt protons while odd-numbered orbits are more exposed to cosmic rays and solar particle events at perigee. This can be seen in the higher proton rates at perigee in Fig. 7 compared with Fig. 6.

Comparisons are made with predictions of inner-belt proton fluxes using the AP8 model as modified in SPENVIS (shown as squares in the figures). Later data obtained in January 1999 are shown for even and odd orbits in Figs. 8 and 9. In Table II, the measured proton fluencies are compared with AP8MAX/SPENVIS predictions for protons of energy greater than 40 MeV. The time period in question is between maximum and minimum but differences for this orbit are only about 3%. In general it can be seen that the predictions are about a factor of two low compared with the observations. A similar underprediction has been noted in [10] and [11] but for much lower orbits below 1000 km.

Both measurements and predictions show the difference between even and odd orbits. Surprisingly the increase in perigee between May 1998 and January 1999 (1212 km to 1502 km)

TABLE II
PROTON FLUENCES > 40 MEV, MEASURED CF SPENVIS PREDICTION

Orbit	Measured Fluence cm-2	AP8-SPENVIS Prediction cm-2
364	1.7×10^7	1.0×10^7
365	1.2×10^7	0.6×10^7
880	1.9×10^7	0.8×10^7
881	1.2×10^7	0.5×10^7

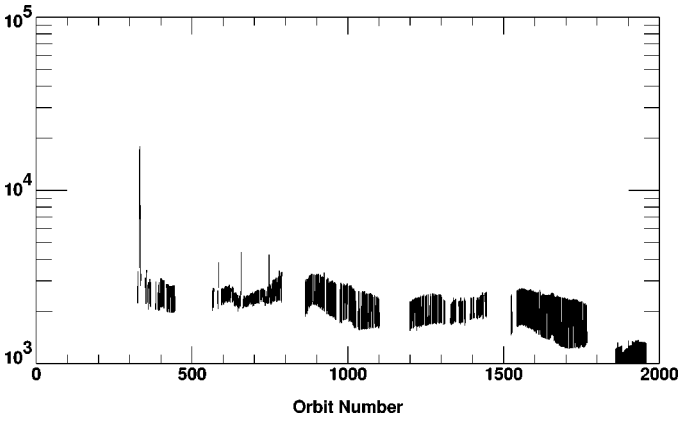

Fig. 10. Time variation of orbit-averaged proton fluxes (>38 MeV) show odd vs even orbit differences and long-term trends due to orbit evolution including increase in perigee height. Orbit 1000 is on March 20, 1999 while orbit 2000 is on July 31, 2000. Note that the plotted data terminate before the increase on July 14, 2000.

is reflected in the drop in predicted fluxes but not in the measured data, which remain almost constant. In general the measured data do show a downward trend with increasing perigee (see Fig. 10). Complete mapping of the count rates into B, L space may shed light on these discrepancies and variations.

2) Temporal Variations: In a previous paper [7], time variations were presented for the period from launch until July 1999. In addition, orbit profiles of count rates were presented for the time period around the solar particle event of August 25, 1998. These illustrated the arrival of significant solar particle fluxes followed by the pumping up of the outer electron belt caused by an ensuing geomagnetic disturbance. In this paper, time variations are extended to July 2000 and the large solar particle event of July 14, 2000 is examined in detail.

Orbit averages of proton fluxes (coincident counts) are presented in Fig. 10 for those orbits in which there are no data gaps. The odd-even orbit differences can be seen while long-term trends are due to orbit evolution, which includes an increase in perigee altitude from 1200 km at the start of the measurements to 2010 km at the end. The spikes are due to the larger solar particle events which can increase the orbit average.

In Fig. 11 orbit-averaged proton fluxes are given for times outside of the radiation belt. The underlying rate is due to cosmic rays and shows a factor two diminution over this time period due to solar modulation. The spikes are due to solar particle events. Several significant events occurred during 1998 and are discussed in the previous paper [7]. Since that time events in 1999 and early 2000 have been relatively small. However the proton flux during the event of July 14, 2000 exceeds that observed

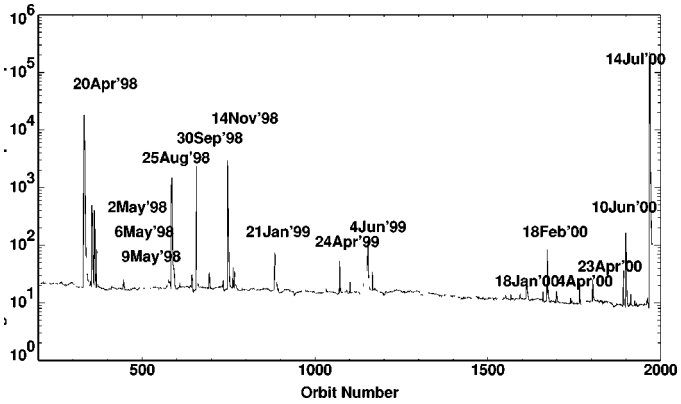

Fig. 11. Orbit-averaged proton fluxes with inner-belt passes removed showing cosmic-ray modulation by a factor two and a number of solar particle events, including the large event on July 14, 2000.

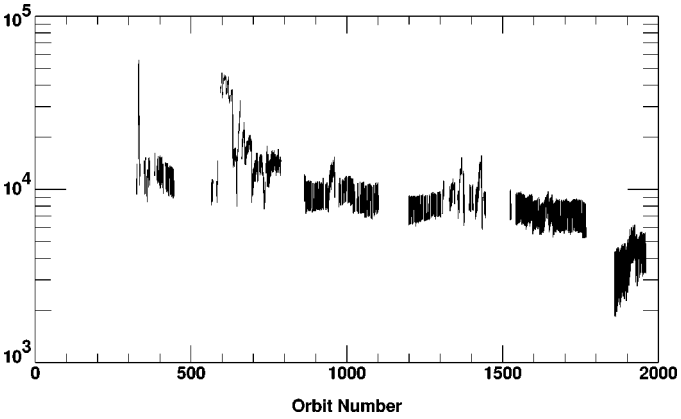

Fig. 12. Orbit-averaged rates in the noncoincident channel show the time variability of electrons.

during events observed previously on MPTB by more than an order of magnitude. This event is discussed in greater detail below.

In Fig. 12, the orbit-averaged rates in the proton singles (noncoincident) channel are presented as a function of time. Besides counting protons, this channel also responds to energetic electrons when fluxes are very high. The large increase at the left hand end of the plot is the April 1998 solar particle event but the following large increases are due to outer-belt electron enhancements. The period between orbits 600 and 700 remains by far the most intense of these and corresponds to late August to October 1998. Smaller increases occurred between February 21 to March 1, 1999, between September 16 and September 23, 1999 and between October 16 and October 21, 1999. Such equinoctial time periods frequently show higher electron fluxes. These electron increases correspond to dose-rate increases in the MPTB dosimeters and the time period between orbits 600 and 700 still contributes most of the accumulated dose in the MPTB experiments beneath 50 mil of aluminum [13].

3) The Solar Particle Event of July 14, 2000: Fig. 11 shows this event to be by far the largest observed on MPTB and GOES data show it to be the largest in solar cycle 23 so far. The responsible solar flare peaked at 1024 UTC on July 14 and created radio blackouts together with a large, fast moving coronal mass ejection. Significant particle increases were first observed

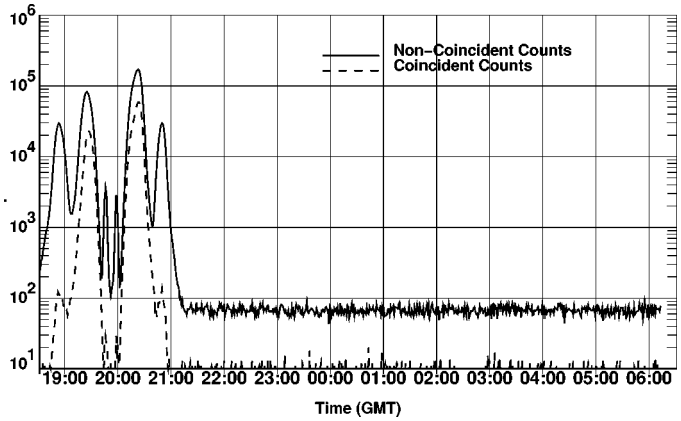

Fig. 13. CREDO count rates for orbit 1966 on July 13 and 14 preceding the solar particle event show relatively low rates of cosmic rays and inner belt protons but significant outer-belt electron fluxes.

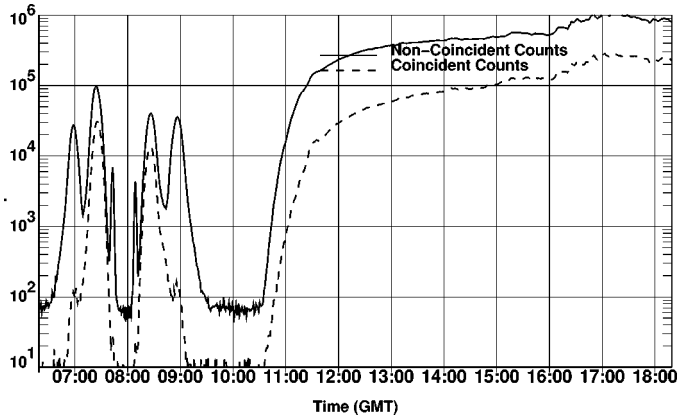

Fig. 14. The solar particle event is seen at 1040 on July 14 during orbit 1967 and rapidly rises to very high levels.

in space at 1040 while ground level neutron monitors recorded a 36% increase [14].

Fig. 13 shows CREDO count rates for the orbit preceding the event The coincident counts measure protons and show two inner-belt passes either side of perigee and then a flat contribution with time due to cosmic rays. It is notable that these fluxes are lower than in the earlier time periods of Figs. 6–9 and reference [7] due to orbit evolution and solar modulation. However the outer electron belt shown in the noncoincident counts is quite intense at this time due to preceding solar activity. Fig. 14 shows the steep increase in count rate at 1040 while Figs. 15 and 16 show that the very high rates continue for more than a day. In addition to the high rates observed outside the belts where geomagnetic shielding is minimal, very large increases are observed at perigee due to its high latitude. The odd-orbit perigee has the higher rates due to its higher L-value as discussed above. The still very high rates observed at even-orbit perigee are indicative of a hard proton spectrum able to penetrate to L-values of three and this is consistent with the observation of a ground level event. By July 16 the rates had decayed by a factor of 100 as shown in Fig. 17. In addition, the geomagnetic storm had severely reduced the outer electron belt.

The integral linear energy transfer (LET) spectra of earlier solar particle events have been presented in reference [7]. These

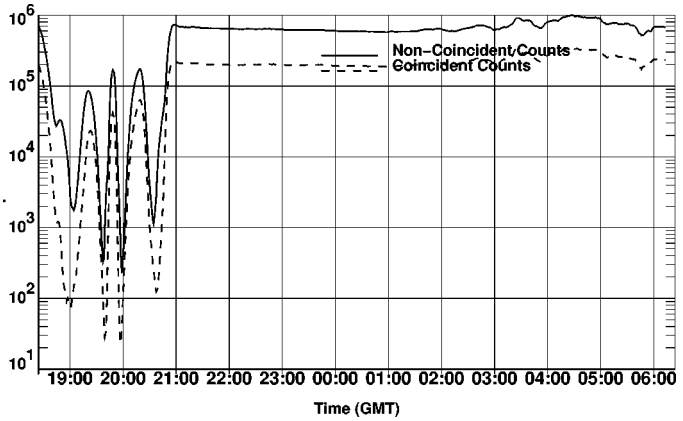

Fig. 15. The high rates are also seen at perigee for the even orbit 1968 on July 14 and 15. This indicates a hard spectrum.

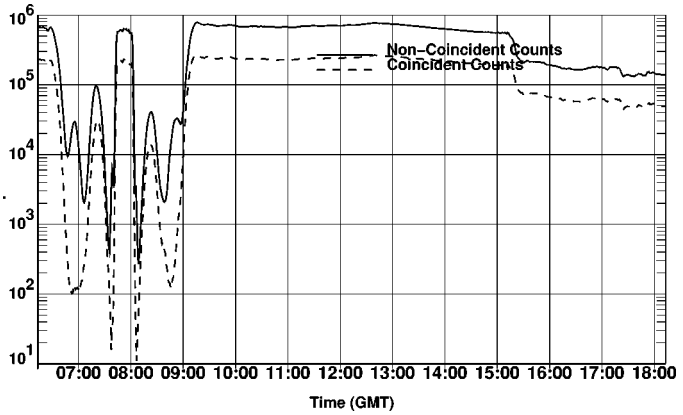

Fig. 16. Count rates for orbit 1969 on July 15 show that high rates are maintained for 1.5 days and odd orbit perigee is fully exposed.

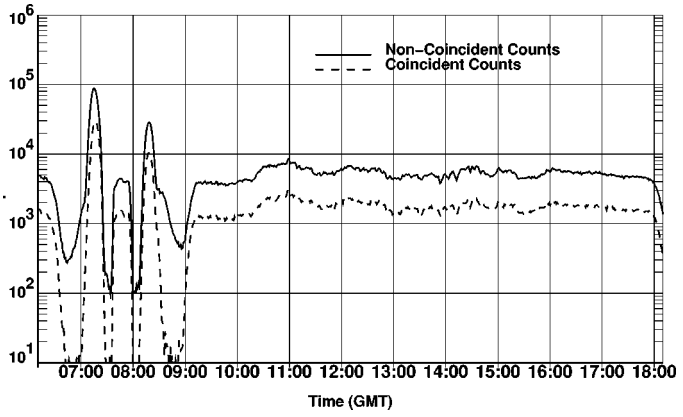

Fig. 17. After 2 days (orbit 1971 on July 16) the solar particle fluxes have dropped by a factor 100. In addition the outer-belt electrons are greatly diminished.

were found to be well below the CREME96 worst week model based on the October 1989 event [15] and showed no increases beyond a LET of 400 MeV/(g cm^{-2}). In Fig. 18 the spectrum is shown averaged over the two peak days of the July 14, 2000 event. It can be seen that this event gives low LET rates from protons of comparable intensity to the October 1989 event. The high LET counts from heavy ions show a very significant increase over quiet time but are not as intense as the CREME96 model.

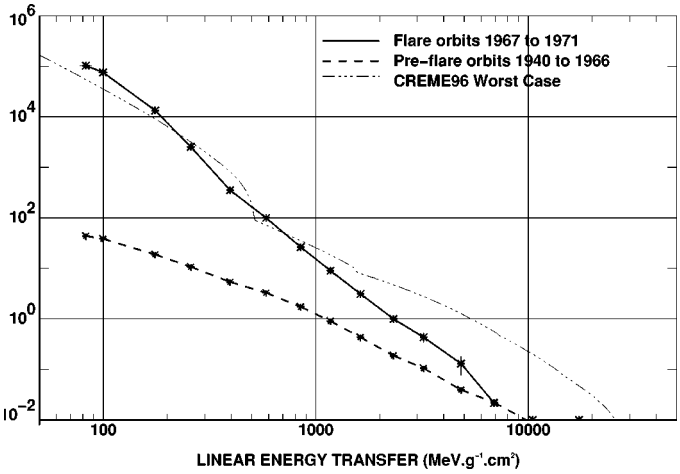

Fig. 18. Integral LET spectra averaged over the 5 peak orbits of the event of July 14, 2000 are compared with spectra from the preceding quiet-time period and the CREME96 worst week model.

IV. Conclusion

For MIR/International Space Station orbit, SAA passes cannot be predicted by using AP8 in conjunction with the updated geomagnetic field. The use of SPENVIS, which rotates the SAA location, gives significant improvement as long as 1-minute time resolution is used.

Dose rates and secondary neutron fluxes observed on MIR are comparable to those observed on Space Shuttle for similar orbits and external cosmic-ray fluxes. The dose from directly ionizing charged particles is reduced by shielding but secondary neutron contributions are surprisingly uniform.

The charge-deposition spectrum is also uniform throughout MIR and shows build-up with respect to minimally shielded SpaceHab locations.

For MPTB in Molniya orbit, two inner-belt proton passes occur in every orbit and these show differences between odd and even numbered orbits due to the different locations of perigee with respect to the radiation belts. A long-term downward trend in inner-belt proton fluxes is due to the increasing altitude of perigee. Fairly good agreement is obtained with AP8 predictions but in general there is a factor 2 underprediction.

The outer-belt electrons are extremely variable in intensity and profile. A large increase following a solar event in late August 1998 corresponds to a large increase in dose-rate observed by other MPTB experiments.

A factor 2 decrease in cosmic-ray fluxes is seen between November 1997 and July 2000 due to solar-cycle modulation.

A number of significant solar-particle events have been observed. Of these the recent event of July 14, 2000 is by far the most intense. This is close to the October 1989 event for protons but would appear to have less heavy ions.

Acknowledgment

R. Haine and C. Caines are thanked for their help in designing and building the CREDO-3 board. The work at DERA is sponsored by the UK Ministry of Defence. J. Ritter and A. Campbell of NRL are thanked for organizing the flight within the MPTB payload. Shuttle flights to MIR were sponsored and organized by BMDO and the DoD Space Test Program. D. Heynderickx is thanked for illuminating discussions on SPENVIS and for allowing alteration of the default time-resolution.

References

[1] C. S. Dyer, A. J. Sims, and C. I. Underwood, "Measurements of the SEE environment from sea level to GEO using the CREAM & CREDO experiments," *IEEE Trans. Nucl. Sci.*, vol. 43, no. 2, pp. 383–402, 1996.

[2] C. Dyer, A. Sims, and C. Underwood, "Radiation belt observations from CREAM and CREDO," in *1996 Geophysical Monograph 97, Radiation Belts: Models and Standards*, pp. 229–236.

[3] C. S. Dyer, P. R. Truscott, C. L. Peerless, C. J. Watson, H. E. Evans, P. Knight, M. Cosby, C. Underwood, T. Cousins, and R. Noulty, "Updated measurements from CREAM & CREDO and implications for environment and shielding models," *IEEE Trans. Nucl. Sci.*, vol. 45, pp. 1584–1599, June 1998.

[4] C. S. Dyer, P. R. Truscott, C. L. Peerless, C. J. Watson, H. E. Evans, P. Knight, M. Cosby, C. Underwood, T. Cousins, R. Noulty, and C. Maag, "Implications for space radiation environment models from CREAM and CREDO measurements over half a solar cycle," *Radiation Measurements*, vol. 30, no. 5, pp. 569–578, Oct. 1999.

[5] J. Adolphsen, J. Barth, E. Stassinopoulos, T. Gruner, M. Wennersten, K. LaBel, and C. Seidleck, "Single event upset rates on 1 M and 256k memories: CRUX experiment on APEX," *IEEE Trans. Nucl. Sci.*, vol. 43, pp. 1964–1974, Dec. 1995.

[6] J. C. Ritter, "Microelectronics and photonics test bed," in *Proc. 20th Ann. AAS Guidance and Control Conference*, 1997, AAS97-024.

[7] C. S. Dyer, C. Sanderson, R. Mugford, C. Watson, and C. Peerless, "Radiation environment of the microelectronics and photonics test bed as measured by CREDO-3," *IEEE Trans. Nucl. Sci.*, vol. 47, pp. 481–485, June 2000.

[8] D. Heynderickx, "Comparison between methods to compensate for the secular motion of the south Atlantic anomaly," *Radiat. Meas.*, vol. 26, pp. 325–331, 1996.

[9] D. Heynderickx, B. Quaghebeur, E. Speelman, and E. Daly, "Space environment information dystem (SPENVIS): A WWW interface to models of the space environment and its effects,", AIAA-2000-0371, 2000.

[10] D. Heynderickx, M. Kruglanski, V. Pierrard, J. Lemaire, M. D. Looper, and J. B. Blake, "A low altitude trapped proton model for solar minimum conditions based on SAMPEX/PET data," *IEEE Trans. Nucl. Sci.*, vol. 46, pp. 1475–1480, Dec. 1999.

[11] S. L. Huston and K. A. Pfitzer, "A new model for the low altitude trapped proton environment," *IEEE Trans. Nucl. Sci.*, vol. 45, pp. 2972–2978, Dec. 1998.

[12] C. E. McIlwain, "Coordinates for mapping the distribution of magnetically tapped particles," *J. Geophys. Res.*, vol. 66, no. 11, p. 3681, 1961.

[13] A. Campbell, "The microelectronics and photonics testbed: Space, ground test and modeling experiments,", RADECS99 Summary Document, N34-38, Sept. 1999.

[14] , http://www.sec.noaa.gov/advisories/bulletins.html, July 17, 2000.

[15] A. J. Tylka, J. H. Adams Jr., P. R. Boberg, B. Brownstein, W. F. Dietrich, E. O. Flueckiger, E. L. Petersen, M. A. Shea, D. F. Smart, and E. C. Smith, "CREME96: A revision of the cosmic ray effects on microelectronics code," *IEEE Trans. Nucl. Sci.*, vol. 44, pp. 2150–2160, Dec. 1997.